eBP: A Wearable System For Frequent and Comfortable Blood Pressure Monitoring From User's Ear

Nam Bui[†], Nhat Pham[†], Jessica Jacqueline Barnitz[†], Zhanan Zou[†], Phuc Nguyen[†], Hoang Truong[†], Taeho Kim[†], Nicholas Farrow[†], Anh Nguyen[†], Jianliang Xiao[†], Robin Deterding[‡], Thang Dinh[§] and Tam Vu[†]

[†]University of Colorado Boulder, [‡]Children's Hospital Colorado, [§]Virginia Commonwealth University

{firstname.lastname}@colorado.edu,Robin.Deterding@childrenscolorado.org,tndinh@vcu.edu

ABSTRACT

Frequent blood pressure (BP) assessment is key to the diagnosis and treatment of many severe diseases, such as heart failure, kidney failure, hypertension, and hemodialysis. Current "gold-standard" BP measurement techniques require the complete blockage of blood flow, which causes discomfort and disruption to normal activity when the assessment is done repetitively and frequently. Unfortunately, patients with hypertension or hemodialysis often have to get their BP measured every 15 minutes for a duration of 4-5 hours or more. The discomfort of wearing a cumbersome and limited mobility device affects their normal activities.

In this work, we propose a device called eBP to measure BP from inside the user's ear aiming to minimize the measurement's impact on users' normal activities while maximizing its comfort level. eBP has 3 key components: (1) a light-based pulse sensor attached on an inflatable pipe that goes inside the ear, (2) a digital air pump with a fine controller, and (3) a BP estimation algorithm. In contrast to existing devices, eBP introduces a novel technique that eliminates the need to block the blood flow inside the ear, which alleviates the user's discomfort.

We prototyped eBP custom hardware and software and evaluated the system through a comparative study on 35 subjects. The study shows that eBP obtains the average error of 1.8 mmHg and -3.1 mmHg and a standard deviation error of 7.2 mmHg and 7.9 mmHg for systolic (high-pressure value) and diastolic (low-pressure value), respectively. These errors are around the acceptable margins regulated by the FDA's AAMI protocol, which allows mean errors of up to 5 mmHg and a standard deviation of up to 8 mmHg.

MobiCom '19, October 21–25, 2019, Los Cabos, Mexico

ACM ISBN 978-1-4503-6169-9/19/10…$15.00

https://doi.org/10.1145/3300061.3345454

CCS CONCEPTS

• **Human-centered computing** → **Mobile computing**; • **Hardware** → *Sensor devices and platforms.*

KEYWORDS

In-ear blood pressure monitoring, In-ear sensing, Frequent blood pressure monitoring, Blood pressure, Wearable devices.

ACM Reference Format:

Nam Bui, Nhat Pham, Jessica Jacqueline Barnitz, Zhanan Zou, Phuc Nguyen, Hoang Truong, Taeho Kim, Nicholas Farrow, Anh Nguyen, Jianliang Xiao, Robin Deterding, Thang Dinh and Tam Vu. 2019. eBP: A Wearable System For Frequent and Comfortable Blood Pressure Monitoring From User's Ear. In *The 25th Annual International Conference on Mobile Computing and Networking (MobiCom'19), October 21-25, 2019, Los Cabos, Mexico.* ACM, NewYork, NY, USA, 17 pages. https://doi.org/10.1145/3300061. 3345454

1 INTRODUCTION

Blood pressure (BP) is one of the foremost vital signs measured when patients first arrive in the hospital, as BP can provide doctors with insight to initiate their diagnosis. For example, chronic kidney disease, sleep apnea, and adrenal and thyroid disorders can all cause high BP, while low BP indicates the possibility of heart or endocrine problems, dehydration, severe infection, or even blood loss. Additionally, uncontrolled elevated BP is a major symptom of many life-threatening diseases, such as hypertension, heart failure or stroke [8]. Until recently, the reliable way to measure BP was

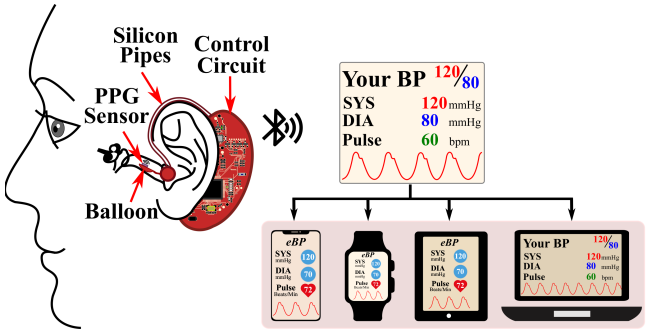

Figure 1: eBP's overview.

done by a health care practitioner (HCP) such as a physician, doctor, or nurse. The clinician wraps an arm cuff around the patient's upper arm and rapidly inflates the cuff with air. Once the cuff has reached maximum inflation, the systolic and diastolic pressures are determined by slowly releasing the air from the cuff and observing the pulse sound with a stethoscope over the brachial artery below the cuff. Since the invention of digital BP devices, non-medical trained users can self-measure their BP at home, as an acoustic sensor can replace the stethoscope, and a pressure sensor with a DC pump can substitute the pressure gauge and hand pump.

However, these devices often cause discomfort and inconvenience for those who need **frequent BP monitoring**, such as hemodialysis (kidney failure) patients [63], individuals with undiagnosed white coat hypertension or undiagnosed masked hypertension [69], which have a prevalence of 15-30% [36] and 16.8% [75] in the US, respectively. There is also an increased use of frequent BP monitoring for post-operative organ transplant recipients [83], with more than 30,000 solid organ transplants occurring every year [74]. In such cases, BP is measured every 30 minutes for 24 hours [31], while each hemodialysis session takes around four hours. Therefore, there is a significant need for an unobtrusive and comfortable BP monitoring approach.

Existing techniques require the blood flow to be blocked completely. Therefore, it causes discomfort when measuring BP frequently. In the case of prolonged dialysis, patients hardly rest because the BP cuff constantly squeezes their arm. The most current BP monitoring devices consist of an arm cuff and a monitor that harnesses around the body, yet this often hinders the wearer's mobility [67]. Therefore, by moving the location of measuring BP to inside the ear, our device has a minimal impact in affecting the users' mobility and comfort.

There have been prior attempts to build a cuff-less, continuous BP monitoring device [13, 105]. Continuous systems rely on the Pulse Transit Time [56] technique, which infers the BP from the time it takes the pulse to propagate from one point to another. It usually measures the time interval between the peaks of the pulse signal and uses reference peaks from an electrocardiogram (ECG). However, these systems are not accurate due to the low specificity ECG on BP. The recent failure of Quanttus is an example [9]. Another cuff-less approach tried capturing BP by pressing on the phone screen [27]. Though this approach is moderately accurate, it requires a user to maintain constant finger pressure in order to obtain a good measurement, which is poorly suited for frequent BP monitoring.

In this paper, we aim to develop a novel wearable system to capture BP inside the ear called eBP as illustrated in Fig. 1. eBP resolves the aforementioned issues with its discreet design, quiet components and convenient location.

eBP's overview: eBP includes (1) a light-based pulse sensor attached to an in-ear inflatable pipe (or balloon), (2) an air pump, a pressure sensor, and a valve controlling module to control the balloon's contact to the in-ear skin for pulse measurement, and (3) a BP estimation algorithm. The in-ear pipe is slowly inflated by the digital pump to create small pressure on the outer ear canal until the diastolic and the systolic value are estimated.

Challenges: Realizing eBP has the following challenges:

(1) In-ear BP monitoring is an unexplored topic in which many of the existing techniques cannot be applied. Even the feasibility of the technique has not been confirmed.
(2) The mechanism enabling the use of an inflatable balloon to measure BP from inside the ear is non-trivial. When the balloon inflates, the sensor should attach firmly to the ear canal and not slide out. In addition, applying insufficient pressure will result in an inaccurate BP measurement, while applying too much pressure may cause discomfort or hurt the ear canal.
(3) The in-ear pulse signals are weak and buried under noises. In addition, the motion artifacts are difficult to remove and can impact BP measurement accuracy.
(4) BP measurements are sensitive to the contact quality (i.e., pressure) between sensor and in-ear skin; yet maintaining consistent contact pressure is difficult.

Contributions: In this paper, we make the following contributions. First, we propose a novel concept of in-ear frequent BP monitoring and show that it is not only feasible but also comfortable. Second, we propose a blocking-free optical-oscillometric approach to allow the in-ear sensor to measure important parameters in BP measurements (i.e., systolic amplitude and diastolic amplitude). Third, we prototype a device with a custom-built circuit and hardware/software components for in-ear BP measurements. In particular, we customize an off-the-shelf catheter to safely insert it into the ear canal with a light pulse sensor attached. In addition, we build a portable in-ear wearable device to control the light pulse sensor and the catheter to capture the pulse signal

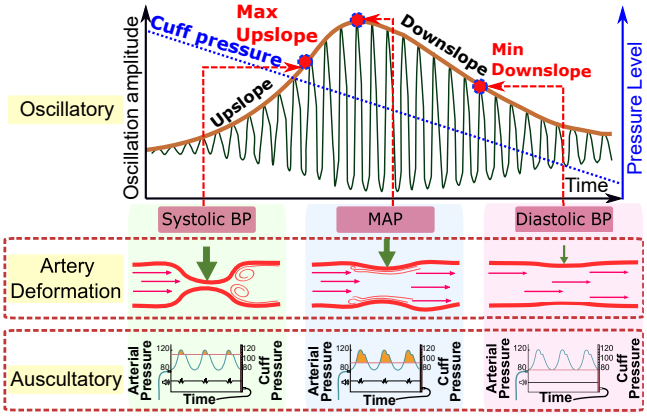

Figure 2: The response of blood artery to outer pressure that causes the measurement of BP.

(i.e, BP) accurately and reliably. Fourth, we devise an algorithm to process and qualify the highly noisy pulse signals captured from inside the ear to ensure the high-quality BP measurements. Lastly, we conduct a study with 35 users and verify the performance of the proposed system using a FDA-approved BP measurement device (KonQuest KBP-2704A).

Applications and Impacts: While eBP is currently a standalone device, with the continued trend of incorporating biometric monitoring into devices [44, 49, 57, 62, 65] that are worn on a daily basis, there would be minimal behavioral changes required on the part of the wearer to benefit from eBP. As ear-worn devices are becoming increasingly popular [3, 6, 59], eBP could potentially be integrated into a headphone or hearing aid, both of which are ubiquitous as the World Health Organization reports that approximately 466 million people worldwide suffer from disabling hearing loss [77] and more than 365 million headphones were sold in 2017 in the US alone [39]. In addition, our proposed BP calculation algorithm can be applied to make existing cuff devices more comfortable. In the case of hardware design, the use of a medical balloon to deliver a sensor into the ear can widely benefit other applications. For example, it can improve the contact points and the conductivity of electrodes for the in-ear sensing area.

2 FUNDAMENTAL OF BP MEASUREMENT

Starting with a brief overview of existing BP monitoring widely in use today, we will point out current limitations, providing context for our novel approach. Measuring blood flow pressure can be done with both invasive or non-invasive methods. Although invasive approaches deliver highly accurate results, it is costly and only available in hospitals. Non-invasive techniques are far more useable, as their process is quick, low cost, and relatively simple. However, these non-invasive techniques are set to cycle or must be done manually, unlike continuous measurements provided by arterial invasive methods.

Artery deformation under the effects of cuff pressure grants the key signatures to estimate BP as shown in Fig. 2. When the cuff pressure is equal to the systolic pressure (SBP), blood flow continues through the occluded artery, but only the highest arterial pressure can be detected. On the other hand, if the cuff pressure is lower than the diastolic pressure (DBP), the detected pulse is very weak. Using auscultatory methods, medical practitioners listen to pulse sound propagation through a stethoscope to determine BP. Oscillatory, on the other hand, was developed for the digital device by estimating BP from the change of pulse amplitude. It detects the Maximum Pulse Amplitude (MAP) A_M first and applies predefined fractions of the peak amplitude ratio A_M/A_S and A_M/A_D to detect where the systolic and diastolic pressure occur and use these values to infer the pressure. A_S and A_D are the amplitude of systole and diastole, respectively. Unlike auscultatory methods, oscillatory methods do not need to completely occlude the blood vessel in order to detect the systolic BP [38], which is well-suited for our balloon model. However, current oscillation ratios are only applicable for the arm or wrist BP measurement model. Therefore, they are not eligible for our in-ear case. Generating a new in-ear ratio requires a large-scale data set, including an invasive method to measure BP from inside the ear, which is infeasible. Instead, we propose a technique to measure BP without applying the characteristic ratios. To achieve this goal, we thoroughly examine the change of amplitude with respect to the change of cuff pressure. Then, we extract the key properties and formulate them into mathematical equations for processing. According to [7], during the deflation:

- Pulse amplitude increases when the cuff pressure is close to the systolic level. The increment increases more quickly when the pressure reaches and passes through the systolic point.
- At the systolic and diastolic cycle cross-section, the amplitude obtains its highest value (the MAP).
- Amplitude rapidly decreases once the pressure passes the MAP and moderately decreases once it reaches the diastole point. In other words, the DBP position occurs at the highest decreasing amplitude.

These observations provide key insights for composing the solutions to detect MAP, SBP, and DBP. In particular, the diastolic position is the minimum of the downslope amplitude, and MAP is the peak of the amplitude, as shown in Fig. 2. We can derive the systolic location as being the maximum of the upslope amplitude. However, sometimes our in-ear balloon pressure might not reach the systolic phase due to comfort requirements. Therefore, we have to rely on the relational

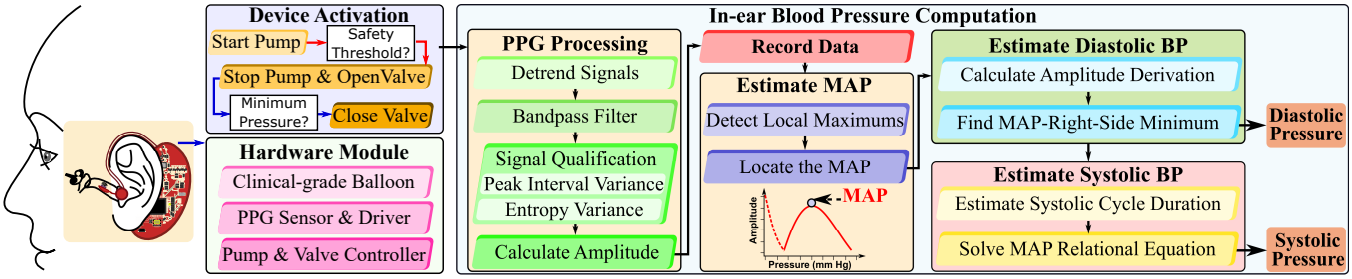

Figure 3: eBP system.

equation between MAP, SBP, and DBP [20]:

$$P_M = \beta P_S + (1 - \beta) P_D, \tag{1}$$

where β is the systole ratio of the cardiac cycle and P_M, P_S and P_D are the MAP, SBP, and DBP respectively. Most literature reports β as a fixed value [52, 58] and is widely accepted, but each person can have a slightly different ratio dependent on age, gender, and health condition. Moreover, an incorrect estimation of β increases the estimation error, as noticed in [64]. In our eBP system, we propose an adaptive estimation for β based on the pulse-wave form.

Realizing the importance of frequent BP monitoring and the discomfort of current devices, we design eBP as ear-worn equipment to (1) capture the pulse signal inside the ear from a balloon-attached pulse sensor and (2) use this information to estimate the BP.

3 EBP'S OVERVIEW

Learning from what was previously mentioned, we designed our system as shown in Fig. 3 to address the challenges. In this section, we explain the goal of our design in detail, the system's components as well as the core algorithms. First of all, there are three essential goals that our design needs to satisfy: (1) allow frequent monitoring with minimal impact on the user's mobility, (2) be comfortable, unobtrusive and easy to use, and (3) obtain a high accuracy BP prediction.

Motivation and challenges for in-ear BP monitoring: Commercialized devices are mostly cumbersome and require a piped cuff be attached to the user's limb, which limits the user's movements. Mounting the sensors onto glasses [13, 45] can significantly improve flexibility, but it may be aesthetically unappealing and highly obtrusive [16]. Therefore, we explore the option of measuring BP from inside the ear for portability, aesthetic appearance, comfort, and social acceptance. Realizing these objectives, many challenges must be overcome.

First, the systolic and diastolic ratio was invented for the arm cuff BP and cannot be adapted directly into our design. Consequently, we propose a new approach to identify the SBP and DBP without using this characteristic fixed ratio.

Second, the traditional approach uses a cuff to compress the artery on the arm or wrist for the pulse measurement. However, this is challenging to repeat inside the human ear, as the in-ear balloon can inflate in any direction, which affects the pulse measurement. Fortunately, by analyzing the human ear anatomy, we found that the two sides of the ear canal are structured differently. In particular, one side (S1) of the canal includes an artery covered by muscles where the pulse signal could be captured while the other side (S2) is right next to a bone. When the in-ear balloon is inflated, the balloon expands and obtains contact with the artery at S1 and does not expand at S2. This mechanism creates a similar environment to the traditional approach used on the arm/wrist; therefore, we can derive an algorithm to measure BP using the amplitude and pressure relationship from pulse measurement theory.

Third, as the balloon inflates and shrinks across multiple measurements, the solution of adhering the pulse sensor to the balloon surface can wear out and be damaged, raising the concern that the sensor can fall off inside the ear. Therefore, we develop a meticulous procedure to attach the sensor by firmly wiring and securing it on the balloon surface.

Fourth, the superficial artery is relatively small compared to the brachial artery. The sensor should face towards the artery in order to obtain a clear pulse signal. However, placing the pulse sensor in the ear is not an easy-handled task, as visibility is restricted. To solve this issue, we develop a pulse-signal qualification model accumulated with our design to precisely justify when the pulse signal is detected.

Last, but not least, hypersensitive skin in ear-canal spurs safety and patient-experience concerns. One-third of the outer ear canal's skin is from 1 to 1.5mm thick, while the inner two-thirds is only 0.1mm in thickness, as shown in Fig. 5. The sensing area mandates our efforts to customize the design by carefully excluding electronic components that have toxic materials or sharp edges.

Proposed solutions:

Non-ratio approach for the calculation of systolic and diastolic BP: Unlike the oscillometric method, we do not apply the fixed-ratio BP because there is no valid

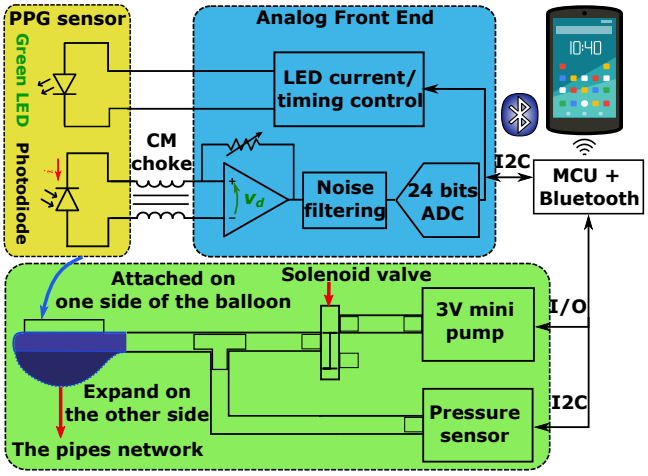

Figure 4: In-ear BP module design.

ratio for inside the ear. For safety purposes, our pressure may not cover the SBP range. Therefore, we aim at estimating the pressure in diastole first according to its minimal downslope amplitude. Then, we substitute the DBP into the MAP-relational equation to estimate the SBP. Moreover, we propose a personalized approach to estimate the systolic fraction β instead of using the common fixed ratio. A thorough explanation of the technique is presented in Section 5.1.

In-ear pulse sensor with the flexible circuit: eBP uses the light-based sensing technique, named Photoplethysmography (PPG) [91], to capture the superficial pulse (BP value). The optical sensor is small and sustainable enough to be attached to the balloon. However, state-of-the-art BP sensing technology is often designed on a printed hard circuit board. When the sensor is placed on the balloon, its surface might create sharp contact, which may hurt the user's ear. We overcome this problem by designing a flexible BP sensing circuit (Section 4.2). This flexible circuit adapts to the balloon's deformation, making the device comfortable to use for a long period of time.

High-quality elastic balloon: The balloon, which serves our specific purpose, needs to satisfy the following criteria: bio-compatibility, safety, high elasticity, consistency, and be strong and resilient to cleaning. To satisfy these conditions, we customize an off-the-shelf medical balloon often used for bladder catheterization (Section 4.2).

In-ear PPG signal qualification: The in-ear PPG power is weaker than that of the finger, wrist, or arm. Therefore, after basic preprocessing, we employ two techniques for signal qualification, including the **Peak Interval Variation** and **Entropy Variance** (Section 6) to eliminate bad data chunks and identify the correct position inside the ear to place the sensor. For conventional signal filtering, we process every 50 milliseconds with DC removal and a bandpass filter. This procedure helps to get rid of noise and other unwanted band signals, to disclose only the pulse waveform. With data that qualifies for this criteria, we calculate their amplitude using our modified peak-to-peak technique.

In-ear PPG signal processing: (1) *Modified peak-to-peak amplitude calculation*: Current peak-to-peak calculation is inconsistent for real-time processing due to the random order of peaks and bottoms. We propose a solution by adding a verification module to ensure the order consistency. (2) *Drift removal for Mean Arterial Pressure detection:* During the first few seconds of the balloon deflating, a large drift away from the calibrated pressure causes the false detection of maximum amplitude. We have developed a solution to detect the MAP based on its local maxima property regardless of the appearance of the drift. (Section 6).

Ear-worn air pump and draining components: Air pump and draining components are designed to inflate and shrink the balloon with predefined configuration. We target the miniaturized components to develop the air pump. The controller will process the signal and detect whether the pressure is sufficient. Then, following the information, it will decide if more air should be pumped in or if the valve should be opened to reduce pressure. The final product will be worn outside the ear. (Section 4.1).

4 SYSTEM HARDWARE DESIGN

4.1 Design considerations

The in-ear BP measuring module consists of three main components: (1) a PPG sensor attached on an in-ear balloon, (2) an air pump and a valve controller to control the balloon having good contact with the in-ear skin, and (3) a central sensing algorithm to compute the PPG value by controlling both the above mentioned two components for robust BP monitoring using an in-ear sensor. The detailed architecture of the module is shown in Fig. 4. Let's discuss the requirements of each component in detail.

The PPG sensor. The PPG sensor consists of a LED (transmitter) shining onto an artery and a photodiode (receiver) capturing the reflected light. Since the human ear canal can be as small as 2.4mm in diameter, both the LED and photodiode need to be miniaturized to fit the ear canal. Second, the artery inside the ear canal is hidden deep below the skin. Thus, the LED in our PPG sensor needs to be bright enough so that the light can deeply penetrate the skin deeper and reach the artery. In addition, the photodiode also needs to be highly sensitive to pick up the small reflected light. Fortunately, the PPG measurement inside the ear does not suffer from the effect of ambient light. In particular, we found that the noise term coming from ambient light can be minimized.

The pump/valve controlling module. To precisely control the air balloon, the pump/valve controlling module needs

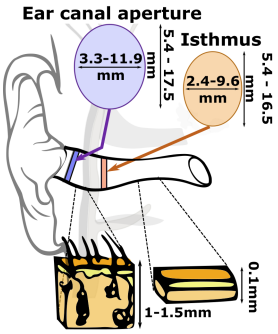

Figure 5: Ear canal anatomy.

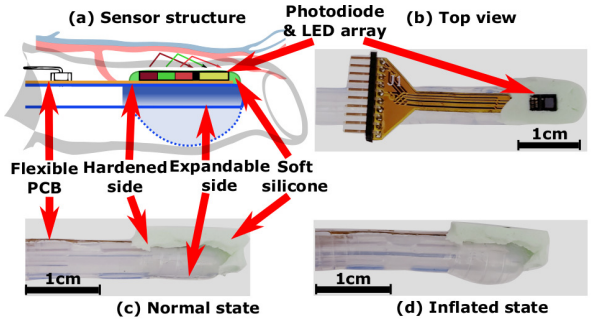

Figure 6: In-ear PPG sensor and balloon design.

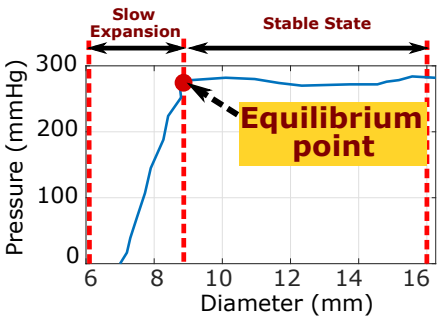

Figure 7: The pressure vs. diameter curve of the balloon.

to ensure the consistency of the contact force for maintaining high-quality PPG measurements. The module includes a digital pressure sensor for measuring the contact force, a mini air pump, a solenoid valve for filling and venting the air and a network of soft silicon pipes connecting them, as illustrated in Fig. 4. When the measurement starts, the mini pump will be activated to fill the balloon with air, and while the valve is closed, the air is kept inside the network. When the PPG sensor has reached the ear canal wall, the pump is stopped, and the balloon is kept in an inflated state for PPG measurement. Pressure values inside the channel are sampled and streamed to our MCU. After the measurement is completed, the valve will be opened to release the contained air and let the balloon return to its normal state.

The in-ear balloon. PPG sensing requires tight contact points between the sensors and the skin for accurate measurement. However, keeping the sensor in contact with the skin at all time might generate discomfort to the user for long-term use. To overcome this challenge, the sensor is designed to be flexible and operates as an in-ear balloon to only contact the human skin tightly when conducting PPG measurements. Specifically, we mount the PPG sensor on top of a small balloon that can be pumped up or vented out via a controller module. Furthermore, the circuit for the PPG sensor needs to deform as the balloon inflates flexibly. It must be engineered on the side of the balloon where it can remain stable as the balloon inflates and deflates.

Since the balloon needs to be inserted into the ear canal, it needs to be carefully designed and must satisfy the following requirements: (1) *bio-compatibility*, it must not contain any substances that could be harmful to the human body in its material; (2) *safety and robustness*, as the balloon needs to sustain a certain amount of air pressure for the measurement and also accommodate various sizes of human ear canals, (3) *user's comfort*, the human ear canal is thin and sensitive; thus, the balloon needs to be soft to make the user feel comfortable while providing enough pressure for our measurement. In addition, as the balloon inflates and shrinks across multiple BP measurements, it needs to have high durability elasticity. Additionally, the inflation and shrinking rate of the balloon needs to be consistent to maintain reliable measurements. Last, but not least, it needs to be strong and resilient to scrubbing when cleaning so that the sensor can be reused multiple times.

4.2 Implementation

Proprietary design of the balloon attaching PPG sensor. We design our in-ear sensor by integrating a PPG sensor with the balloon of a Foley catheter made by POIESIS MEDICAL [15], as illustrated in Fig. 6. The Foley catheter is created from 100% medical silicon so it can be safely and comfortably inserted inside the body [15]. We found that SFH7050 PPG sensor from OSRAM [2] is the best fit for the small size of the ear canal. It has the size of 4.7 mm x 2.5 mm x 0.9 mm and performs highly accurate measurements due to its special design for the crosstalk blocking technique [2]. The PPG sensor includes a super-bright green LED transmitter, having the wavelength of 525 nm, which is a commonly used wavelength in PPG measurement. The receiver is a sensitive photodiode that captures the reflected lights from the LED transmitter, and infers PPG values. Section 5 describes the algorithm to calculate PPG in detail. The sensor is driven by a specialized analog front end IC (AFE4404) [1] from TI. This AFE provides an accurate built-in LED driver and a timing controller, an ultra-low noise trans-impedance amplifier with a wide-range programmable gain, and a precision 24-bit ADC to control the SFH7050 sensors. To ensure high fidelity signals, a common-mode (CM) choke coil is used as an analog low-pass filter before the input of the AFE. It helps to suppress CM noises induced by electromagnetic interference over the wires between the sensor and the AFE. The digital data from the AFE is then streamed to our MCU (MSP430F5529) [14] through I2C communication with a sampling rate at 320 Hz.

Our in-ear balloon is hardened, so it will only expand on one side. The other side must be kept stable for the mounted LEDs and photodiode. The PPG sensor is soldered on a thin

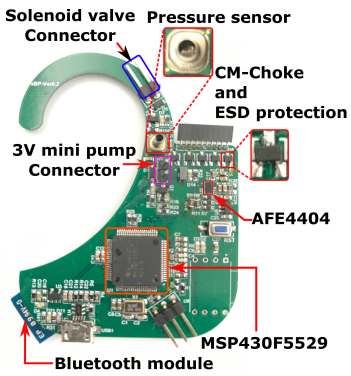

Figure 8: eBP hardware.

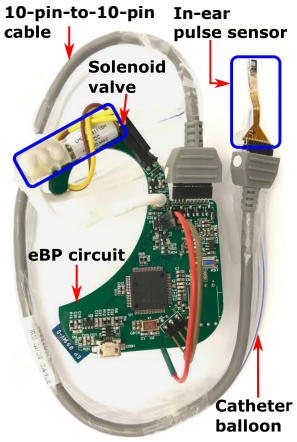

Figure 9: eBP prototype.

layer (0.1 mm) of flexible PCB. The PCB is then integrated on top of the balloon catheter by using a thin layer of liquid silicone gel. After curing for one hour at 80^{o}C, the bonding between the PPG sensor and catheter surface becomes hardened and stays robust. Furthermore, to make the sensing unit more comfortable inside the ear, we coated Smooth-On Ecoflex 00-30 soft silicone [5] around the edge of the sensor, covering all sharp corners. The surface of the sensor was kept flat by using a glass slide, which is removed once the Ecoflex is cured. Thus, the flat surface of the sensor offers a better sensing ability.

The price of a catheter balloon and the SFH7050 PPG sensor are $16.99 and $2.82, respectively. In total, manufacturing a disposable in-ear balloon sensor costs approximately $19.81, which is cheaper than a disposable BP handcuff [4, 12]. The cost can be reduced further through large-scale production.

In-ear balloon pressure monitoring. In literature, it has been shown by experiments that the relationship among pressure inside the balloon, its volume, and diameter are nonlinear [60]. Especially when the diameter is in the range from 7 mm to 9 mm inside the ear canal, the pressure has an initial peak called the equilibrium point accompanied by a slow balloon expansion as the constituent polymer makeup of the balloon is altered. After the balloon has reached its equilibrium point, the pressure inside the balloon will keep stable or reduce, even if its volume increases. Fig. 7 shows the relationship between the pressure and diameter of the silicone-based balloon used in our study, which matches the results in existing studies [29, 60]. As a result, we cannot rely on pressure values to know whether the balloon has reached the wall of the ear canal or not. Instead, the quality of PPG signals is observed and the pump will be stopped when we observe clear PPG signals.

In addition, an over-threshold protection mechanism is implemented to stop pumping air when the pressure inside the balloon is over the threshold. Since the size of each person's ear canal is different, with its diameters in the range from 2.4 to 17.5 mm, we want to continuously and slowly inject the air until one side of the balloon touches the skin of the user's ear canal and partially blocks the artery. However, the balloon also has its limit as to how much air it can hold. Thus, we do not want to inject too much air into it, making it permanently deformed or causing it to burst. From the balloon datasheet [15] and an experimental burst test in [60], the failure pressure of the silicone-based balloon is between 15 and 20 psi. Thus, the pressure inside the balloon is continuously monitored by the MSP430 MCU and the pump will be stopped if the pressure reaches more than 10 psi, as a rule of thumb. This addresses the challenge of different ear canal sizes while maintaining the safety of our system.

Concerning safety, we use the Ecoflex soft silicone design across our evaluation, including a few trials at the beginning. This is because the diameter of the balloon when expanding inside the ear canal does not exceed the break-out point of the silicone gel. When the diameter of the inflated balloon is larger than 30 mm, we start seeing some cracks on the silicon at the connection between the Ecoflex and the balloon. Since the ear canal diameter is only from 7mm to 9mm, which is much smaller than the cracking point, the balloon is safe to be inflated inside the ear.

Central processing controller. The central controller as shown in Fig. 8 is responsible for (1) communicating to mobile devices through Bluetooth to receive commands and report sensing data, (2) driving the analog front-end IC to collect the PPG measurement to the sensor, and (3) controlling the pump/valves to control the balloon pressure for accurate PPG measurement. Overall, Fig. 9 presents the eBP prototype depicting the integration of the in-ear pulse sensor with the main module.

Power consumption. All components in our designed module are chosen to operate with low power consumption and also have small sizes. These are very important in a "wearable" scenario where the user still has mobility when they wear the device, whereas it is not possible with a conventional cuff-based BP measuring devices. Additionally, less power consumption, in turn, will reduce the capacity of the Li-Po battery, which is the main limiting factor to minimize the weight of our designed module. During the measurement, the MCU, AFE, pressure sensor, and Bluetooth module consume at maximum of only 4.6 mA, 325 uA, 1.7 mA, and 30 mA, respectively. The LED transmitter, valve, and mini pump draw 10 mA, 110 mA, and 150 mA. Thus, our module consumes around 303 mA while the BP measurement is running. On the other hand, only 4.95 mA is drawn when our measurement is not running. Thus, a 400 mA Li-Po battery is used, providing up to 1.3 hours of continuously measurement, which is equivalent to roughly 80

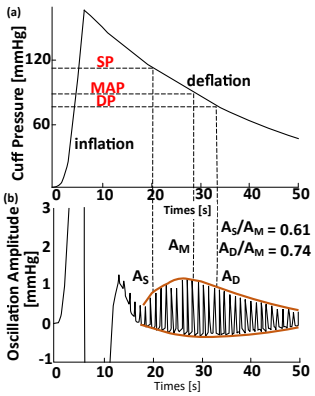

Figure 10: Amplitude vs. Pressure [54].

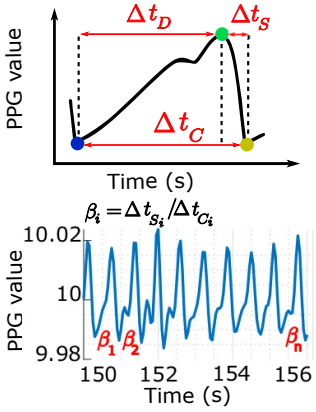

Figure 11: Systolic fraction β detection.

measurements. However, running the device all the time is not practical or necessary. Instead, the users usually only need to measure their BP a few times per day. If the system is not running any measurement, it can last for more than 2 days (53 hours) in an idle state.

5 IN-EAR BLOOD PRESSURE ESTIMATION ALGORITHMS

This section presents the algorithm to **measure the systolic BP with a partially blocked artery, which does not depend on the fixed-BP ratio**. In conventional oscillometry, after detecting the MAP as the highest pulse amplitude (A_M) (Fig. 10 (b)), the peak amplitude fractions are applied to estimate the location of systolic amplitude (A_S) and diastolic amplitude (A_D). From [54], the ratio of A_S and A_M is 0.61, whereas the ratio between the A_D and A_M is 0.74. However, this ratio is not consistent, as [32, 53] reports them to be 0.55 and 0.85 respectively. In addition, these ratios are for the arm cuff BP monitoring devices. Moreover, deriving an in-ear oscillation ratio requires a huge data set and an invasive method for measuring BP from inside the ear as a reference. Our method is independent of the ratio and does not completely occlude the artery. In fact, the pressure only needs to be slightly higher than MAP. eBP determines the MAP and DBP first, from direct measurements and then infers SBP indirectly.

5.1 Systolic BP Measurement

To estimate the SBP (P_S) given the pressure of MAP (P_M) and diastole (P_D), we apply Eq. 1, where β is the systole ratio of the cardiac cycle. Most literature reports β as a fixed value [52, 58] and this is widely accepted, but, it is developed for the brachial artery, not for the artery inside the ear. In our eBP system, we propose an adaptive estimation for β. To achieve

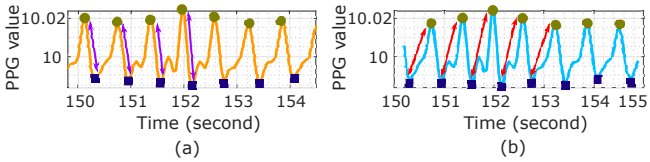

Figure 12: Illustration of the inconsistency of conventional peak-to-peak computation.

this goal, we first explain the derivation of the Eq. 1. By considering one PPG cycle, we can formulate MAP as follows: $P_M = \sum_{i=1}^{n} P(i)/n$ in discrete form or $P_M = \frac{1}{\tau}\int_0^{\tau} P(t)dt$ in continuous form. By assuming systole belongs to the interval $(0, \tau\beta)$ and diastole is from $(\tau\beta, \tau)$, P_M is the total pressure average of systolic and diastolic pressure.

$$P_M = \frac{1}{\tau}\int_0^{\tau\beta} P(t)dt + \frac{1}{\tau}\int_{\tau\beta}^{\tau} P(t)dt \tag{2}$$

Then, we multiply the first term and second term by β and $1-\beta$ respectively.

$$P_M = \beta\left[\frac{1}{\tau\beta}\int_0^{\tau\beta} P(t)dt\right] + (1-\beta)\left[\frac{1}{\tau(1-\beta)}\int_{\tau\beta}^{\tau} P(t)dt\right] \tag{3}$$

$\frac{1}{\tau\beta}\int_0^{\tau\beta} P(t)dt$ is the average of SBP and $\frac{1}{\tau(1-\beta)}\int_{\tau\beta}^{\tau} P(t)dt$ is the average of DBP. Eq. 1 is equivalent to Eq. 3 by substituting $P_S = \frac{1}{\tau\beta}\int_0^{\tau\beta} P(t)dt$ and $P_D = \frac{1}{\tau(1-\beta)}\int_{\tau\beta}^{\tau} P(t)dt$. In one cycle, we detect the peak and two bottom points, and then subtract their position in sequence as shown in Fig. 11. Δt_D, Δt_S and t_C are the duration of diastolic, systolic and the whole cycle respectively. The systolic fraction is $\beta = \Delta t_S/\Delta t_C$. Given a frame of n cycles, we can compute β by averaging all β_i in the frame. Since our system runs in real-time, we only collect the first 10 cleanest frames to estimate the systolic fraction.

However, we first need to determine MAP and DBP prior to estimate the SBP. Their estimation procedures are described in the following sections.

5.2 Mean Arterial Pressure Detection

MAP represents the pulse pressure or the highest PPG amplitude. The precise location depends on the quality of the amplitude. In this section, we reveal the issue of using peak-to-peak to calculate the amplitude of a real-time data and propose our improvement. In addition, sometimes, a sharp drift occurs when switching from inflation to deflation. The drift's amplitudes are higher than that of the real MAP, leading to a false detection problem. We also present our solution to address the issue of drift in this section.

Amplitude calculation: To compute the peak-to-peak amplitude of a window sample containing multiple pulses, conventional wisdom calculates the amplitude every cycle

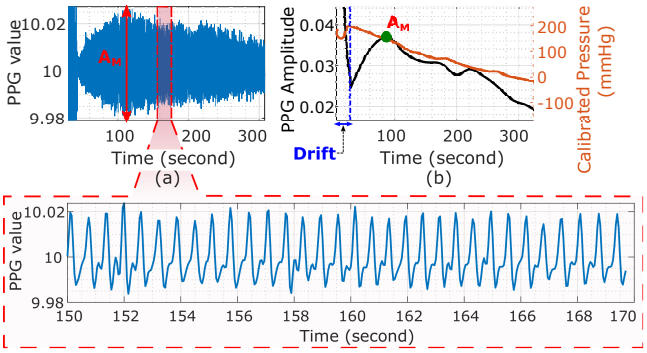

Figure 13: In-ear PPG signal (a) with corresponding amplitude and pressure (b).

and averages them. Fig. 12 (a) demonstrates when the first peak appears before the first bottom, then, the amplitude is calculated by subtracting the peak to the right-side bottom. However, when the bottom occurs first, the left-side bottom is subtracted as shown in Fig. 12 (b). Since the appearance of peak or bottom is variable, the amplitude obtained from each frame is inconsistent. To obtain a unique calculation, we omit the first bottom so that Fig. 12 (b) can convert into Fig. 12 (a). Let $P = \{p_i, i = \overline{1,n}\}$ and $B = \{b_i, i = \overline{1,m}\}$ represent the position sets of peaks and bottoms of the PPG signal X, respectively. The amplitude of each cycle, denoted as amp_i, can be derived consistently as follows:

$$amp_i = \begin{cases} X(p_i) - X(b_i), & p_i < b_i \\ X(p_i) - X(b_{i+1}), & otherwise \end{cases} \quad (4)$$

Fig. 13 (a) demonstrates the PPG signal variation with respect to reducing pressure. The bottom panel displays a PPG signal sample from 150^{th} to 170^{th} seconds. Fig. 13 (b) shows the corresponding amplitude using the peak-to-peak method.

Drift Removal: To detect the correct MAP point instead of ones belonging to the drift, we impose an additional criteria leveraging the local maxima property. Specifically, MAP is not only the maximum amplitude point, it also indicates the pulse amplitude transient state of increasing to decreasing as shown in Fig. 10 [54] and 13. In contrast, points within the drift are not local maximums. Therefore, we employ the following steps to precisely detect the MAP.

(1) Detect pulse amplitude's local maximums. This step confirms the removal of points belonging to the drift.
(2) The highest value of local maximums corresponds to the MAP location.

5.3 Diastolic BP Measurement

Since the oscillation ratios cannot be applied to eBP, we propose a non-ratio method to estimate the DBP. When the pressure passes the MAP point, it will reach the point of

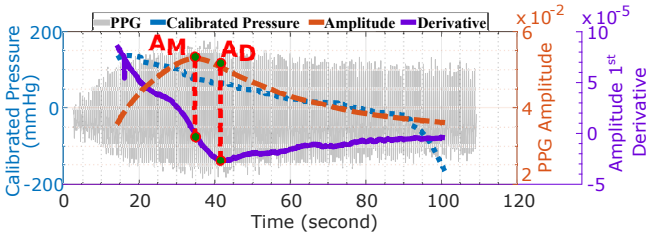

Figure 14: First derivative of PPG amplitude discloses diastolic BP.

Algorithm 1: PPG signal Entropy Variance

input : x /* Current window signal with n samples */
B /* List of bottom indices */
output: vS /* Variance Entropy of current window */

```
ls ← []; /* List entropy */
for each sample b_i in B do
    u ← getSubSignal(x,b_i, b_{i+1}); ls[i]← calcEntropy(u);
vS ← calcVariance(ls);
return vS;
```

diastole that yields the following unique signature: according to [7], amplitude rapidly decreases once the pressure passes the MAP and moderately decreases once it reaches the diastole point. In other words, the DBP position occurs at the highest decreasing amplitude. We can formulate this as the minimum of the first derivative amplitude. Fig. 14 illustrates this idea. The dashed orange line represents the PPG amplitude, the solid purple is the first derivative, the dotted blue depicts the calibrated pressure, and the gray one is the PPG signal. In this example, the drift does not occur, thus the MAP is the local maxima of the amplitude, which corresponds to the 0 point of the first-order derivative. After the MAP, a rapid decrease is observed until the 43^{rd} second, which corresponds to the minimal first order derivative and indicates the location of DBP.

6 PPG QUALIFICATION AND SIGNAL PROCESSING

Due to the sensitivity of the pulse signal inside the ear, we propose a set of criteria to qualify the correct pulse shape. This criterion serves to remove non-pulse data chunks and detect the correct location to measure BP. In this section, we also present key signal processing techniques. We process the recording signal in real-time using a sliding window of approximately 4 seconds with 90% overlap. Before extracting the BP measurement, we pre-process each window as follows:

Signal Qualification. Our signal qualification aims to omit non-pulsatile data and movement noise from the user and the in-ear sensor probe:

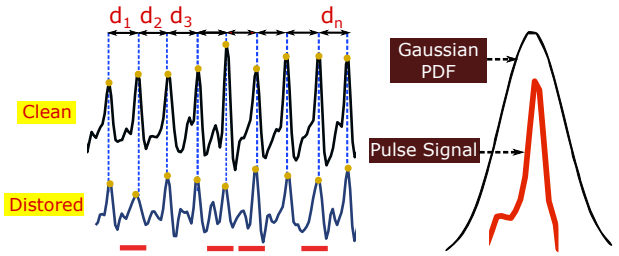

Figure 15: Peak Interval Variance versus Entropy variance.

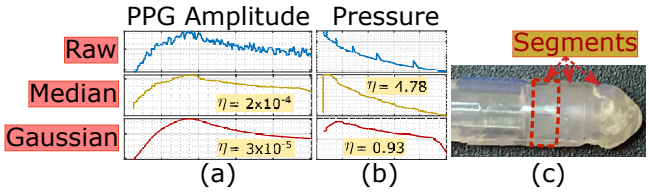

Figure 16: Results of median and Gaussian smoothing filter on amplitude (a) and pressure trend (b), and the balloon structure (c).

Peak Interval Variability (PIV): The ideal PPG signal has a fixed peak-to-peak interval, however, as the PPG signal is quasi-periodic there is the interval variability. The PIV is calculated as the standard deviation of all peak intervals in the current window. In normal conditions, the PIV falls under a certain threshold. However, the sensor is prone to movement noise, which disrupts the PPG trend and the corresponding peak interval. This leads to a drastic change in the peak-to-peak intervals with increasing PIV, which informs us that the current processing window is contaminated by noise. In our application, a PIV threshold of 1.1 is sufficient to detect the distortion.

Entropy variance: The PIV qualifies the pulse signal based on quasi-periodic properties. This is sufficient to calculate the heart rate, but inadequate to compute the PPG amplitude. Consider the two data chunks in Fig. 15, both the clean and distorted signals have similar PIV scores when their peaks almost overlap each other. However, the distorted signal peak height, or amplitude, is inconsistent. The red underline marks non-pulse shaped signals. Therefore, a rule is needed that restricts the signal based on the pulse shape for our motion elimination model. Among different techniques, entropy can classify pulse waveform [28, 90, 97] by quantifying how much the signal probability density function differs from a uniform distribution. The entropy S of a signal x is defined as $S(x) = -\sum_{i=1}^{n} x[i]^2 log_e(x[i]^2)$ that correlates to the change in signal shape. A chunk of PPG data is clean whenever all pulses have similar entropy. In other words, the variance of entropy should be smaller than a threshold of 230 that, according to our experiment, is the minimum value to have a clean and stable PPG signal. Algorithm 1 summarizes the estimation of a PPG signal entropy window. Given a window signal with n samples and a bottom indices list, we isolate each pulse by collecting data between b_i and b_{i+1}. The entropy is calculated for all extracted pulses and stored in a list ls. Finally, we obtain the entropy variance by computing the variance of ls.

We propose two metrics, including Peak Interval Variability and Entropy variance to assess the signal quality. The PPG signal is considered clean data if it satisfies both criteria and will be processed to estimate BP.

Bandpass Filter. We apply the finite impulse response (FIR) bandpass filter in the 0.42-3.33 Hz range to obtain the PPG amplitude. The PPG peak is essential to predict the amplitude and BP, which occurs between 0.42Hz and 3.33 Hz corresponding to the human heart rate range of 25 to 200 beat-per-minutes [10].

Gaussian Filter. High frequency noise present in PPG amplitude can corrupt the true location of MAP and diastole, thereby increasing the error rate. A comparison between Gaussian and Median filtering [92] is conducted to identify the optimal amplitude smoothing technique. To quantify the granularity level η, we use the standard deviation of differences $\eta = \sigma(\frac{dx}{dt})$ with x as the interested signal. Fig. 16 (a) shows that Gaussian filtering is more fine-grained than Median filtering. In particular, the granularity level η of Gaussian filtered signals is one order of magnitude higher than the Median kernel, thereby, confirming our choice. We compute the Gaussian kernel h via the following equation: $h[i] = e^{-(i-w_h/2)^2/2\sigma_h^2}, i = \overline{1, w_h}$, where w_h is the filter size and $\sigma_h = w_h/5$.

Pressure Spikes Correction: During deflation, pressure changes should yield a linear trend. However, the balloon's structure is composed of multiple segments (Fig. 16 (c)), which induces a faster contraction when crossing the border between segments. This event causes spikes on the pressure deflation raw signal, as shown in Fig. 16 (b). Unlike the amplitude, there is minimal difference between the two filtering approaches granularity score (Fig. 16 (b)). Therefore, we use the Median filter to address those spikes, as small drifts are still observed at either end following Gaussian filtering.

PPG Peak Detection. Each heartbeat interval creates one local peak, which can be differentiated using a peak detection algorithm within each predefined non-overlapping subwindow. A signal sample s_i is considered as a peak, if it is the maximum of that window.

Up until this point, we have described the complete system design. In the following section, we present our system performance through an intensive evaluation.

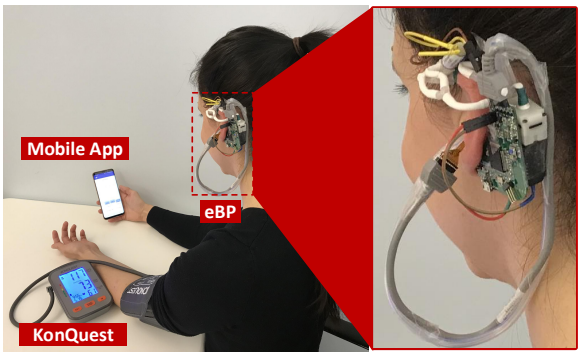

Figure 17: Experiment setup to compare eBP with the KonQuest device.

7 EVALUATION

In this section, we present the set of experiments conducted to evaluate the overall performance of eBP and demonstrate the feasibility of using our BP device frequently in daily life. We first present the key results of performing BP measurements using the eBP system. Then, we evaluate different factors that can affect eBP's performance. Finally, we analyze the users' experience survey when using eBP

7.1 Experimental Methodology

We obtained the IRB approval to conduct experiments for the evaluation of eBP. The participant demographics is shown in Table 1. We tested eBP alongside an FDA-approved, gold standard, arm-cuff BP measurement device (KonQuest KBP-2704A [11]) (Fig. 17). For assessment, we use the metric that is widely accepted by other BP studies, which consist of bias or mean error μ, a precision or standard deviation (SD) σ error and a Pearson correlation coefficient ρ.

This experiment is tested on participants of both genders and various ages. eBP participants place the in-ear balloon inside their ear. Next, the cuff of the KonQuest device is wrapped around the upper arm of each participant. We simultaneously measure the BP of each participant from our Android app running on the Samsung Galaxy S9 and the gold standard BP device. This process is repeated twice and takes about twenty minutes. We sterilize our device with an alcohol wipe, between each experiment, by softly cleaning the balloon tip and sensor. During the experiment, the participant has to sit still to ensure the BP reading is correct. In addition, the balloon needs to be mounted in the right position so that it will not fall out. It turns out that only the P2 location in Fig. 22 (a) can hold the sensor properly because the tragus helps to keep the sensor tight.

Table 1: Demographic description of participants

Demographic data of study population	
Age (years)	18 - 35 years old
Blood Pressure	Systolic: 93-146 , Diastolic: 53-113
Gender Ratio	Male: 24, Female: 11

7.2 System Performance

In this section, we evaluate eBP performance and showcase the comparative results between eBP and the KonQuest KBP-2704A.

Fig. 18 shows the Bland-Altman diagram that describes the average error between eBP and the ground-truth. Consequently, the mean and SD error of SBP and DBP are 1.8 mmHg and 3.1 mmHg, which is within the Association for the Advancement of Medical Instrumentation's (AAMI) requirement (μ_{AAMI}<5 mmHg) [94]. In addition, our SD error for SBP and DBP also satisfy the criteria where σ_{AAMI}<8 mmHg [94]. On the other hand, Fig. 19 displays the Pearson correlation coefficients of SBP and DBP measurements by eBP and the KonQuest device. We select five participants data for calibration using a polynomial regression model. There were some error cases where the measurement was performed without taking sufficient stability. For example, the balloon fell out of the ear because of sweat, movement, or the ear canal was too narrow. When the balloon falls out, there is no valid pulsatile waveform detected. As a result, the system cannot predict the BP, thus, providing no data for the evaluation. The correlation shown of 0.81/1.0 for the SBP and 0.76/1.0 for the DBP represents that our system's prediction is highly correlated to that of the FDA approved device.

7.3 Power consumption

We measure the power consumption of both eBP hardware module and eBP app (installed on a Samsung Galaxy S9) in two scenarios: (1) during BP measurement and (2) without BP measurement. eBP hardware module power consumption is measured using Monsoon Power Monitor. eBP app power consumption is measured using AccuBattery application. Note that the power measurement of eBP hardware is done in 1 minute, while it takes 9 minutes to obtain a reliable measurement from AccuBattery app. eBP hardware consumes 1279.28mW and 31.34mW during BP measurement and without BP measurement, respectively. eBP app consumes 1406 mW and 1119 mW during eBP measurement and without BP measurement, respectively. In summary, eBP hardware consumes 1247.94 mW (1279.28 mW - 31.34 mW) to operate the pump, the valve, the LED, and the microcontroller. eBP app consumes 287 mW (1406 mW - 1119 mW) for BP calculation.

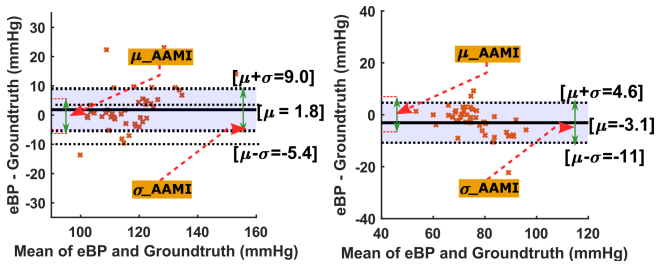

(a) SBP (b) DBP

Figure 18: Bland-Altman plot comparing eBPś measurements and groundtruth .

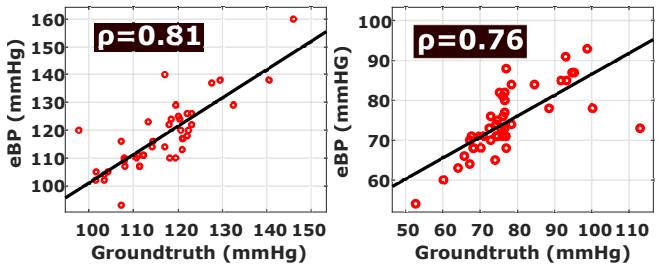

(a) SBP (b) DBP

Figure 19: Pearson correlation coefficients of eBPś estimation and groundtruth.

7.4 Prediction Stability

We conducted experiments to verify the robustness of our calibration procedure based on polynomial fitting. We replicated the process by taking 250 randomly picked times from the learning set. Finally, we explore the frequencies of mean and SD error as shown in Fig. 20. Overall, the highest frequencies of both SBP and DBP mean error falls between 4-5 mmHg which satisfies AAMI standards. Similarly, the highest frequency of SD errors is less than 8mmHg which also qualifies the AAMI protocol. In addition, 9 out of 35 candidates proceed 10 times of data collection to calculate the intraclass correlation coefficient (ICC). Fig. 21 shows the ICC result of each candidate. The average ICC of SBP and DBP are 0.8 and 0.76, respectively.

7.5 Optimal sensor location

In this section, we evaluate PPG signal quality when being captured from inside the ear. Fig. 22 (a) illustrates the 4 most common positions our sensors are located. We collect 10 seconds of data from each participant separately from the main test for this evaluation. Fig. 22 (b) shows that the signal power is highest at position P2 on the left side.

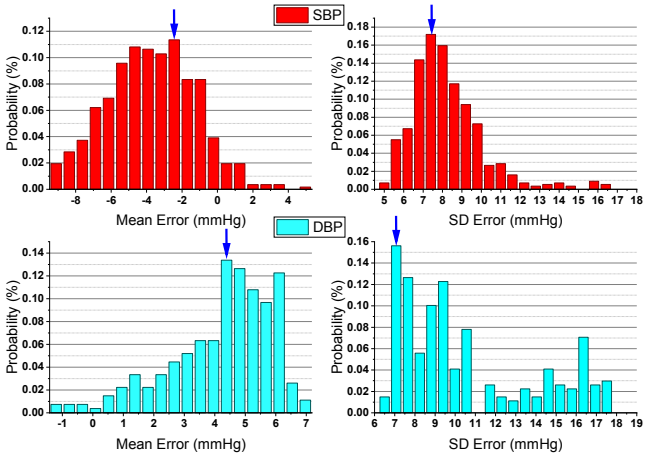

Figure 20: Mean and SD error in cross validation.

7.6 User Experience Survey

We asked participants (students and school staffs) who participated in the study to complete a questionnaire on their experience with the eBP once the experiment was complete. The survey included questions on the users' perspective of eBP's convenience, portability, ease of use, and a comparison of eBP to the digital device. The survey uses a rating scale from 1 to 5 corresponding with "Very Unsatisfied" to "Very Satisfied".

After we explained how to use eBP to record a BP measurement, users were then asked to place the device inside their ear. As shown in Fig. 23, more than 60% of the users reported that they were satisfied or highly satisfied that they could easily use eBP by themselves. As this experiment was the first time all participants had their BP measured from inside their ear some users were initially confused about the operating procedure eBP. We believe that after repetitive use people would be more comfortable using eBP by themselves. Additionally, 65% of the users found eBP's portability to be satisfactory or very satisfactory. The results also show that more than 80% of the users were satisfied or very satisfied with the convenience of eBP. When the participants compared the use of eBP alongside the commercial digital BP device, 75% of the users considered eBP easier to use. Overall, participants agree with the novelty of measuring BP in the ear and were satisfied with eBP. However, there were 3 cases where users reported a little scratch due to the soft silicone falling off. Also, 7 out of 35 participants did not like the noise when the balloon partially slides out of the ear canal during an inflated state.

8 DISCUSSION

Optimizing the balloon design: Our current off-the-shelf medical balloon shape does not respond linearly to pressure

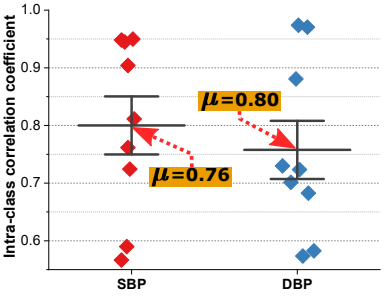

Figure 21: Intraclass correlation coefficient of eBP and groundtruth.

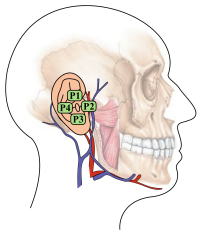

(a) Setup

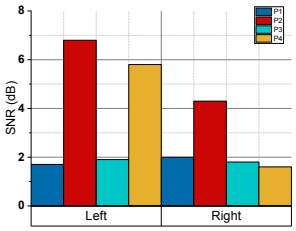

(b) SNR

Figure 22: The SNR of PPG signals at different sensor locations.

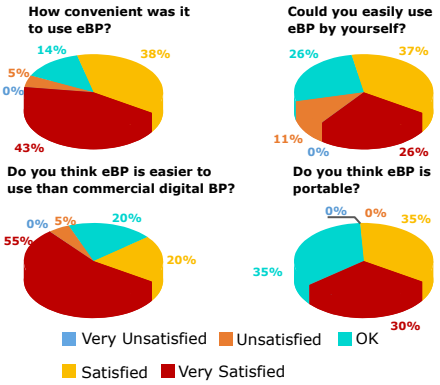

Figure 23: User experience questionnaire results.

changes, which causes several issues. One of these is the appearance of spikes, mentioned in Sec. 5, that we can remove with median filtering. Since the balloon's intended purpose is a urinary catheter, it has a high level of stiffness and thus demands a strong pressure to break the equilibrium point. In addition, unlike the cuff, the elasticity of the balloon quickly recoils to its original state at the onset of deflation. Therefore, it inserts a large amount of pressure into the pressure sensor that sometimes overwhelms the device. As a result, improving the linearity of the balloon's material is our priority. The new material should satisfy the linearity property whilst being comfortable, but still complying with the safety requirement as the current catheter balloon does.

Sensor placement: Changing the location of the PPG sensor inside the ear can affect the signal quality and system performance. Therefore, first of all, a better tragus-mounting mechanism is required to keep the sensor stable inside the ear. Then, SNR, PIV, and entropy variance are utilized to evaluate the signal quality of different sensor placement locations to obtain the cleanest signal.

High idle current draw: The idle current draw is 4.95 mA. 92% (4.6 mA/4.95 mA) of this value is consumed by the microcontroller, which is still running in its active mode. It is possible to further reduce the current draw, which can be as low as 2.1 uA, by using the standby mode of the microcontroller.

Leveraging on-chip processing data: Continuously streaming raw data over Bluetooth requires a significant amount of power (30 mA). This consumed power can be minimized by off-loading signal processing to the microcontroller and taking advantages of the dedicated DSP core. Therefore, on-chip processing can be utilized to lessen power consumption, which leads to smaller battery usage and hence reduce the size and weight of the device.

Miniaturizing the ear-worn circuit: The size of the current eBP prototype is not optimal. Therefore, design optimization, including the use of smaller components and reducing power consumption is required to miniaturize the eBP's main circuit.

Systole ratio estimation in atrial fibrillation (AF): Our system needs a correct estimation of systolic ratio in the cardiac cycle to calculate BP. Therefore, when the pulse is irregular as in an AF patient, it can affect the accuracy of the eBP measurement. Moreover, the system might not be able to return a BP result due to the failure of getting a stable estimation of systolic ratio. One possible solution is to reduce the window size and increase the number of selected cleanest frames, e.g. 100 so that it has more chances to capture clean data. In addition, a specific triggering mechanism needs to be designed to update the number of cleanest frames when atrial fibrillation patient is detected. Further studies with clinical IRB are required to understand the performance on AF patients.

Large scale evaluation: Currently, eBP is evaluated on 35 participants from our institution. To explore the system further, a more extensive study with a large number of participants and patients should be conducted.

Safety control and monitoring: So far, we configure a safety threshold for the pressure and use a low power DC pump to protect users. However, this solution only prevents the air from pumping into the balloon continuously. We also need a mechanism for supervising the eBP placement to ensure that users do not place it too deep inside their ear.

9 CONCLUSION

In this paper, we presented eBP a new method to capture BP from inside the ear, that measures the artery BP from the superficial artery near the ear canal. Existing techniques

which measure BP on the arm or wrist cannot be applied to measure BP from inside the ear as the require fixed systolic and diastolic detection ratios. We developed our model to estimate the in-ear BP by observing the behavior of pulse amplitude. Therefore, no constant parameters are required in our proposed model. In this paper, we also introduce a technique to customize an off-the-shelf catheter to become our in-ear pulse pressure sensor. We built custom hardware and software for eBP and evaluated the system through a comparative study on 35 subjects. The study shows that eBP obtains an average error of 1.8 mmHg and -3.1 mmHg and standard deviation error of 7.2 mmHg and 7.9 mmHg for systolic (high-pressure value) and diastolic (low-pressure value), respectively. These errors are within the acceptable margins regulated by FDA's AAMI protocol, which allows average BP difference of up to 5 mmHg and standard deviation of up to 8 mmHg. This promising results not only show the feasibility of an in-ear blood monitoring concept but also open up the possibility of making current gold standard cuff-based BP measurement more comfortable.

10 RELATED WORKS

Measuring blood flow pressures can be separated into two categories: invasive and non-invasive. Although invasive approaches are only used in clinical settings when continuous BP monitoring is medically necessary [26, 34], as it is expensive and inconvenient. Furthermore, there is potential for wave reflection at the catheter tip [48] when inserting the catheter into the artery [89, 96]. Thus, expertise is required for invasive methods and therefore used as the ground-truth for non-invasive validation [30, 46, 78].

There are several non-invasive methods: auscultation (sphygmomanometry) [22, 81, 101], ultrasound [24, 85], oscillometric [38, 87, 102, 106], photoplethysmographic (PPG) [35, 66, 95], and palpatory [82, 86]. Originally, the mercury sphygmomanometer was the gold standard for official BP measurement. However, the mercury ban has led to an increase in non-mercury devices [70, 76].

Auscultatory is the traditional method to measure BP. It is often performed in clinical settings to measure the Korotkoff sounds that resemble SBP and DBP, at the onset and disappearance of the sounds respectively. However, it requires medical training and if clinical guidelines are not followed, the results can be inaccurate [61]. Automating the auscultatory method uses an acoustic sensor to measure the Korotkoff sounds. But it requires a quite environment to obtain accurate measurements as the microphone is susceptible to noise [108].

To determine BP using Doppler ultrasound technique, a transmitter and receiver are placed under a sphygmomanometer cuff. As the cuff deflates, a Doppler shift occurs when SBP moves against the arterial wall and when this movement stops DBP is recorded [76]. Usually, ultrasound BPs occur when more vascular system information is needed [103].

The oscillometric method is used in automatic devices and ambulatory settings. Oscillating vibrations are emitted when a fully inflated cuff starts to deflate, where the onset and disappearance of the vibrations closely resemble SBP and DBP [23]. This method uses empirically derived algorithm and thus BP is an estimate [47]. Also, motion artifacts affect this method [76].

To measure BP with PPG sensors, Penaz finger-cuff attaches a PPG under the cuff to detect the arterial pulsation and drive a servo-loop to maintain the equality of external pressure and internal artery pressure [76]. The SBP and DBP are obtained from the external oscillations. Yet, this method yields inaccurate BP measurements when there are peripheral vasoconstriction or vasodilation and movement noise [50, 73].

Recently, smartphone-based BP monitoring has increased as most smartphones have a PPG sensor [37, 55] and while convenient, it does require continuous finger pressure. On the other hand, Wang et al. [104] introduce the combination of smartphone built-in camera and accelerometer to measure BP. Researchers have also explored the feasibility of using the finger [27, 33, 51], wrist [79, 99], leg [21], ankle [25, 88, 107], toe [80, 84, 98], and eye [13, 17, 43]. The finger is not recommended due to the effect of limb position on BP [72, 73]. A wrist device yields inaccurate measurements if not held at heart level [71]. The leg and ankle are used in special cases like below-knee amputation healing or peripheral arteriosclerotic disease, respectively. Measuring BP at the toe is uncomfortable and generally for specific cases. The eye is a difficult to get an accurate BP, so related papers have focused on hypertension.

Similar to eBP, others studied the ear as a place to measure blood flow pressure, measuring on the earlobe [41, 93] or tragus [18, 42]. Existing studies have used a microphone to detect blood flow [40], a time delay between two ears [68], a sealed air chamber between the end of the earplug and the eardrum [19], and a light-emitting element for irradiating a living body part [100]. Even though these works explain the device design or the system structure, they do not prove the device performance by comparing to gold standard data.

ACKNOWLEDGMENTS

We thank the shepherd and the anonymous ACM MobiCom reviewers for their insightful comments. This research is partially supported by NSF CNS/CSR 1846541, NSF SCH 1602428, Google Faculty Awards 2018, the Schramm Foundation and the Colorado Advanced Industries Accelerator (AIA).

REFERENCES

[1] [n.d.]. AFE4404: Ultra-Small Integrated AFE for Wearable, Optical Heart-Rate Monitoring and Biosensing. https://tinyurl.com/yy88eu5n.

[2] [n.d.]. BioMon Sensor SFH7050, Osram Opto Semiconductors. https://tinyurl.com/y7g6yrbn.

[3] [n.d.]. The Complete Guide to Hearable Technology in 2019. https://tinyurl.com/y3hdvr8e.

[4] [n.d.]. Disposable NIBP Cuff. https://tinyurl.com/y4gojld8.

[5] [n.d.]. Ecoflex 00-30, Smooth-On. https://tinyurl.com/y77pfgnun.

[6] [n.d.]. The future is ear: Why "hearables" are finally tech's next big thing. https://tinyurl.com/y9y6yeln.

[7] [n.d.]. Guest Commentary: How blood-pressure devices work. https://tinyurl.com/y5rmewuf.

[8] [n.d.]. HBP and the Cardiovascular System. https://tinyurl.com/ybv4vlst.

[9] [n.d.]. Health-Tracking Startup Fails to Deliver on Its Ambitions. https://tinyurl.com/hxtudnt.

[10] [n.d.]. Know Your Target Heart Rates for Exercise, Losing Weight and Health. https://tinyurl.com/yauzz8hm.

[11] [n.d.]. KONQUEST KBP-2704A. https://tinyurl.com/y4njpa4s.

[12] [n.d.]. Medline Disposable Vinyl BP Cuff with Marquette Connector, 2-Tube, Adult, 5/bx. https://tinyurl.com/y46u38z4.

[13] [n.d.]. Microsoft Files Patent for Eyeglasses That Measure Blood Pressure. https://tinyurl.com/yazqxqjo.

[14] [n.d.]. MSP430F5529: 25 MHz MCU with Integrated USB Phy, 128KB Flash, 8KB RAM, 12Bit/14 Channel ADC, 32BIT HW Multiplier. https://tinyurl.com/qa5lyoe.

[15] [n.d.]. Poiesis Medical DuetteTM Dual-Balloon 2-way Urinary Catheter. http://www.poiesismedical.com/products/duette/.

[16] [n.d.]. Why Google Glass Failed And Why Apple Watch Could Too. https://tinyurl.com/y6mpvaqp.

[17] Audrey Adji. 2018. Eye Clinic as a Potential Site to Measure Blood Pressure. *American journal of hypertension* (2018).

[18] Kimihisa Aihara, Shoichi Hayashida, Shinji Mino, Hiroshi Koizumi, Naoe Tatara, Taisuke Oguchi, and Junichi Shimada. 2011. Blood pressure meter. US Patent 7,963,923.

[19] Arie Ariav. 2006. Ear probe particularly for measuring various physiological conditions particularly blood pressure, temperature and/or respiration. US Patent App. 11/373,280.

[20] P. D. Baker, D. R. Westenskow, and K. Kück. 1997. Theoretical analysis of non-invasive oscillometric maximum amplitude algorithm for estimating mean blood pressure. *Medical and Biological Engineering and Computing* 35, 3 (01 May 1997), 271–278.

[21] Robert W Barnes, GD Shanik, and EE Slaymaker. 1976. An index of healing in below-knee amputation: leg blood pressure by Doppler ultrasound. *Surgery* 79, 1 (1976), 13–20.

[22] Gareth Beevers, Gregory YH Lip, and Eoin O'Brien. 2001. Blood pressure measurement: Part I-Sphygmomanometry: factors common to all techniques. *Bmj* 322, 7292 (2001), 981–985.

[23] Abi Berger. 2001. Oscillatory Blood Pressure Monitoring Devices. *BMJ : British Medical Journal* 323 (October 2001), 919.

[24] I. F. Black, N. Kotrapu, and H. Massie. 1972. Application of Doppler ultrasound to blood pressure measurement in small infants. *The Journal of pediatrics* 81, 5 (1972), 932–935.

[25] Frank E Block and G Todd Schulte. 1996. Ankle blood pressure measurement, an acceptable alternative to arm measurements. *International journal of clinical monitoring and computing* 13, 3 (1996), 167–171.

[26] W. W. Butt and H. Whyte. 1984. Blood pressure monitoring in neonates: comparison of umbilical and peripheral artery catheter measurements. *The Journal of pediatrics* 105, 4 (1984), 630–632.

[27] Anand Chandrasekhar, Chang-Sei Kim, Mohammed Naji, Keerthana Natarajan, Jin-Oh Hahn, and Ramakrishna Mukkamala. 2018. Smartphone-based blood pressure monitoring via the oscillometric finger-pressing method. *Science translational medicine* 10, 431 (2018), eaap8674.

[28] R. R. Coifman and M. V. Wickerhauser. 1992. Entropy-based algorithms for best basis selection. *IEEE Transactions on Information Theory* 38, 2 (March 1992), 713–718.

[29] Troy J Cross, Sophie Lalande, Robert E Hyatt, and Bruce D Johnson. 2015. Response characteristics of esophageal balloon catheters handmade using latex and nonlatex materials. *Physiological reports* 3, 6 (2015).

[30] F. H. Ding, W. X. Fan, R. Y. Zhang, Q. Zhang, Y. Li, and J. G. Wang. 2011. Validation of the noninvasive assessment of central blood pressure by the SphygmoCor and Omron devices against the invasive catheter measurement. *American journal of hypertension* 24, 12 (2011), 1306–1311.

[31] P. E. Drawz, M. Abdalla, and M. Rahman. 2012. Blood pressure measurement: clinic, home, ambulatory, and beyond. *American journal of kidney diseases : the official journal of the National Kidney* 60, 3 (April 2012), 449–462.

[32] G. Drzewiecki, R. Hood, and H. Apple. 1994. Theory of the oscillometric maximum and the systolic and diastolic detection ratios. *Annals of Biomedical Engineering* 22, 1 (01 Jan 1994), 88–96.

[33] J Eckstein, T Burkardt, C Winterhalder, L Leonardi, E Thommen, S Weber, R Birkemeyer, A Seeck, N Koenig, and M Doerr. 2017. P441Use of a smartphone camera to estimate systolic blood pressure compared to standard oscillometric blood pressure measurement-a prospective trial. *European Heart Journal* 38, suppl_1 (2017).

[34] Langesaeter Eldrid, Leiv Arne Rosseland, and Audun Stubhaug. 2008. Continuous Invasive Blood Pressure and Cardiac Output Monitoring during Cesarean Delivery: A Randomized, Double-blind Comparison of Low-dose versus High-dose Spinal Anesthesia with Intravenous Phenylephrine or Placebo Infusion. *Anesthesiology: The Journal of the American Society of Anesthesiologists* 109, 5 (2008), 856–863.

[35] G. Fortino and V. Giampà. 2010. PPG-based methods for non invasive and continuous blood pressure measurement: an overview and development issues in body sensor networks *(IEEE Medical Measurements and Applications Proceedings (MeMeA))*. 10–13.

[36] S.S. Franklin, L. Thijs, T.W. Hansen, E. O'Brien, and J.A. Staessen. 2013. White-Coat Hypertension: New insights from recent studies. *Hypertension* 62, 6 (December 2013), 982–987.

[37] Aman Gaurav, Maram Maheedhar, Vijay N Tiwari, and Rangavittal Narayanan. 2016. Cuff-less PPG based continuous blood pressure monitoring-A smartphone based approach. In *Engineering in Medicine and Biology Society (EMBC), 2016 IEEE 38th Annual International Conference of the*. 607–610.

[38] L. A. Geddes, M. Voelz, C. Combs, D. Reiner, and C. F. Babbs. 1982. Characterization of the oscillometric method for measuring indirect blood pressure. *Annals of Biomedical Engineering* 10, 6 (01 Nov 1982), 271–280.

[39] GfK. 2019. *Global unit sales of headphones and headsets from 2013 to 2017 (in millions)*.

[40] Albrik Levick Gharibian. 2016. Smart blood pressure measuring system (SBPMS). US Patent App. 14/757,077.

[41] Waldemar Greubel, Albrecht AC Von Muller, Hubertus Von Stein, and Rudolf Wieczorek. 1993. Method of continuous measurement of blood pressure in humans. US Patent 5,237,997.

[42] Yoshiyuki Habu, Kouji Hagi, Hitoshi Ozawa, Kimihisa Aihara, Naoe Tatara, Shinji Mino, and Hiroshi Koizumi. 2008. Blood Pressure Measuring Apparatus and Blood Pressure Measuring Method. US Patent App. 11/664,690.

[43] Sohan Singh Hayreh. 1996. Systemic arterial blood pressure and the eye. *Eye* 10, 1 (1996), 5.

[44] Josiah Hester, Travis Peters, Tianlong Yun, Ronald Peterson, Joseph Skinner, Bhargav Golla, Kevin Storer, Steven Hearndon, Kevin Freeman, Sarah Lord, Ryan Halter, David Kotz, and Jacob Sorber. 2016. Amulet: An Energy-Efficient, Multi-Application Wearable Platform. In *Proceedings of the ACM Conference on Embedded Networked Sensor Systems*. 216–229.

[45] Christian Holz and Edward Wang. 2017. Glabella: Continuously Sensing Blood Pressure Behavior using an Unobtrusive Wearable Device. *Interactive, Mobile, Wearable and Ubiquitous Technologies* (September 2017), 23.

[46] Ivan G. Horvath, Adam Nemeth, Zsofia Lenkey, Nicola Alessandri, Fabrizio Tufano, Pal Kis, Balazs Gaszner, and Attila Cziraki. 2010. Invasive validation of a new oscillometric device (Arteriograph) for measuring augmentation index, central blood pressure and aortic pulse wave velocity. *Journal of hypertension* 28, 10 (2010), 2068–2075.

[47] Gary James and Linda Gerber. 2018. Measuring arterial blood pressure in humans: Auscultatory and automatic measurement techniques for human biological field studies. *American Journal of Human Biology* 30 (January 2018).

[48] H. Kanai, M. Iizuka, and K. Sakamoto. 1970. One of the problems in the measurement of blood pressure by catheter-insertion: Wave reflection at the tip of the catheter. *The Journal of pediatrics* 8, 5 (1970), 483–496.

[49] Fahim Kawsar, Chulhong Min, Akhil Mathur, Marc Van den Broeck, Utku Günay Acer, and Claudio Forlivesi. 2018. eSense: Earable Platform for Human Sensing. In *Proceedings of the 16th Annual International Conference on Mobile Systems, Applications, and Services*. 541–541.

[50] N. Kizilova. 2018. Review of emerging methods and techniques for arterial pressure and flow waves acquisition and analyses. *International Journal of Biosen Bioelectron* 4, 4 (April 2018), 179–187.

[51] Tuula Kurki, N Ty Smith, Norman Head, Hollis Dec-Silver, and Angela Quinn. 1987. Noninvasive continuous blood pressure measurement from the finger: optimal measurement conditions and factors affecting reliability. *Journal of clinical monitoring* 3, 1 (1987), 6–13.

[52] Soojeong Lee, Gwanggil Jeon, and Gangseong Lee. 2013. On Using Maximum a Posteriori Probability Based on a Bayesian Model for Oscillometric Blood Pressure Estimation. *Sensors (Basel, Switzerland)* 13 (10 2013), 13609–23.

[53] Jiankun Liu, Hao-Min Cheng, Chen-Huan Chen, Shih-Hsien Sung, Mohsen Moslehpour, Jin-Oh Hahn, and Ramakrishna Mukkamala. 2016. Patient-Specific Oscillometric Blood Pressure Measurement. *IEEE Transactions on Biomedical Engineering* 63, 6 (2016), 1220–1228.

[54] Jiankun Liu, Jin-Oh Hahn, and Ramakrishna Mukkamala. 2012. Error Mechanisms of the Oscillometric Fixed-Ratio Blood Pressure Measurement Method. *Annals of biomedical engineering* 41 (11 2012).

[55] J. Liu, B. Yan, Y. Zhang, X. R. Ding, S. Peng, and N Zhao. 2018. Multi-wavelength Photoplethysmography Enabling Continuous Blood Pressure Measurement with Compact Wearable Electronics *(IEEE Transactions on Biomedical Engineering)*. 1–12.

[56] M. Lokharan, K. C. Lokesh Kumar, V. Harish Kumar, N. Kayalvizhi, and R. Aryalekshmi. 2017. Measurement of Pulse Transit Time (PTT) Using Photoplethysmography. In *The 16th International Conference on Biomedical Engineering*, James Goh, Chwee Teck Lim, and Hwa Liang Leo (Eds.). Springer Singapore, 130–134.

[57] D. Looney, P. Kidmose, C. Park, M. Ungstrup, M. L. Rank, K. Rosenkranz, and D. P. Mandic. 2012. The In-the-Ear Recording Concept: User-Centered and Wearable Brain Monitoring. *IEEE Pulse* 3, 6 (2012), 32–42.

[58] M. Mafi, S. Rajan, M. Bolic, V. Z. Groza, and H. R. Dajani. 2012. Blood pressure estimation using maximum slope of oscillometric pulses. In *2012 Annual International Conference of the IEEE Engineering in Medicine and Biology Society*. 3239–3242.

[59] Vinaya Manchaiah, Brian Taylor, Ashley L. Dockens, Nicole R. Tran, Kayla Lane, Mariana Castle, and Vibhu Grover. 2017. Applications of direct-to-consumer hearing devices for adults with hearing loss: a review. *Clinical Interventions in Aging* 12 (2017), 859–871.

[60] John M Mathis, John D Barr, Charles A Jungreis, and Joseph A Horton. 1994. Physical characteristics of balloon catheter systems used in temporary cerebral artery occlusion. *American journal of neuroradiology* 15, 10 (1994), 1831–1836.

[61] D.W. McKay. 2008. Measuring blood pressure: a call to bare arms? *CMAJ : Canadian Medical Association journal = journal de l'Association medicale canadienne* 178, 5 (February 2008), 591–593.

[62] N. Merrill, M. T. Curran, J. Yang, and J. Chuang. 2016. Classifying mental gestures with in-ear EEG. In *2016 IEEE 13th International Conference on Wearable and Implantable Body Sensor Networks (BSN)*. 130–135.

[63] Dana C. Miskulin and Daniel E. Weiner. 2017. Blood Pressure Management in Hemodialysis Patients: What We Know And What Questions Remain. *Seminars in Dialysis* 30, 3 (2017), 203–212.

[64] Daniel Moran, Yoram Epstein, Gad Keren, Arie Laor, Jack Sherez, and Yair Shapiro. 1995. Calculation of Mean Arterial Pressure During Exercise as a Function of Heart Rate. *Applied human science : journal of physiological anthropology* 14 (12 1995), 293–295.

[65] Anh Nguyen, Raghda Alqurashi, Zohreh Raghebi, Farnoush Banaeikashani, Ann C. Halbower, and Tam Vu. 2016. A Lightweight and Inexpensive In-ear Sensing System For Automatic Whole-night Sleep Stage Monitoring. In *Proceedings of the 14th ACM Conference on Embedded Network Sensor Systems CD-ROM*. ACM, 230–244.

[66] M. Nitzan, A. Patron, Z. Glik, and A. T. Weiss. 2009. Automatic noninvasive measurement of systolic blood pressure using photoplethysmography. *Biomedical engineering online* 8, 1 (2009), 28.

[67] Mion Junior D. Nobre, F. 2016. Ambulatory Blood Pressure Monitoring: Five Decades of More Light and Less Shadows. *Arquivos brasileiros de cardiologia* 106, 6 (June 2016), 528–537.

[68] James A Nolan and Trevor J Moody. 1999. Method and apparatus for continuous non-invasive monitoring of blood pressure parameters. US Patent 6,004,274.

[69] Eoin O'Brien. 2003. Ambulatory blood pressure monitoring in the management of hypertension. *Heart* 89, 5 (2003), 571–576.

[70] E. O'Brien. 2003. Demise of the mercury sphygmomanometer and the dawning of a new era in blood pressure measurement. *Blood pressure monitoring* 8, 1 (2003), 19–21.

[71] Eoin O'Brien, Roland Asmar, Lawrie Beilin, Yutaka Imai, Jean-Michel Mallion, Giuseppe Mancia, Thomas Mengden, Martin Myers, Paul Padfield, Paolo Palatini, et al. 2003. European Society of Hypertension recommendations for conventional, ambulatory and home blood pressure measurement. *Journal of hypertension* 21, 5 (2003), 821–848.

[72] Eoin O'Brien, Neil Atkins, and Jan Staessen. 1995. State of the market: a review of ambulatory blood pressure monitoring devices. *Hypertension* 26, 5 (1995), 835–842.

[73] E O'Brien, B Waeber, G Parati, J Staessen, and MG Myers. 2001. European Society of Hypertension recommendations on blood pressure measuring devices. *Bmj* 322 (2001), 532–536.

[74] Department of Health and Human Services. 2018. *Organ Donation and Transplantation*.

[75] G. Ogedegbe, C. Agyemang, and J. E. Ravenell. 2010. Masked hypertension: evidence of the need to treat. *Current hypertension reports* 12, 5 (October 2010), 349–355.

[76] G. Ogedegbe and T. Pickering. 2010. Principles and techniques of blood pressure measurement. *Cardiology clinics* 28, 4 (2010), 571–586.

[77] World Health Organization. 2018. *Deafness and hearing loss.*

[78] Christian Ott, Siegberto Haetinger, Markus P Schneider, Matthias Pauschinger, and Roland E Schmieder. 2012. Comparison of two noninvasive devices for measurement of central systolic blood pressure with invasive measurement during cardiac catheterization. *The Journal of Clinical Hypertension* 14, 9 (2012), 575–579.

[79] Gianfranco Parati, Roland Asmar, and George S Stergiou. 2002. Self blood pressure monitoring at home by wrist devices: a reliable approach? *Journal of hypertension* 20, 4 (2002), 573–578.

[80] A Pérez-Martin, G Meyer, C Demattei, G Böge, J-P Laroche, I Quéré, and M Dauzat. 2010. Validation of a fully automatic photoplethysmographic device for toe blood pressure measurement. *European Journal of Vascular and Endovascular Surgery* 40, 4 (2010), 515–520.

[81] D. Perloff, C. Grim, J. Flack, E. D. Frohlich, M. Hill, M. McDonald, and B. Z. Morgenstern. 1993. Human blood pressure determination by sphygmomanometry. *Circulation* 88, 5 (1993), 2460–2470.

[82] Fabio Procacciante, Pietro Picozzi, Massimo Pacifici, Stefania Picconi, Sandro Ruggeri, Aldo Fantini, and Nicola Basso. 2000. Palpatory method used to identify the recurrent laryngeal nerve during thyroidectomy. *World journal of surgery* 24, 5 (2000), 571–573.

[83] G. V. Ramesh Prasad. 2012. Ambulatory blood pressure monitoring in solid organ transplantation. *Clinical Transplantation* 26 (December 2012), 185–191.

[84] DE Ramsey, DA Manke, and DS Sumner. 1983. Toe blood pressure. A valuable adjunct to ankle pressure measurement for assessing peripheral arterial disease. *The Journal of cardiovascular surgery* 24, 1 (1983), 43–48.

[85] A. K. Reddy, G. E. Taffet, S. Madala, L. H. Michael, M. L. Entman, and C. J. Hartley. 2003. Noninvasive blood pressure measurement in mice using pulsed Doppler ultrasound. *Ultrasound in medicine biology* 29, 3 (2003), 379–385.

[86] Dinesh Sahu and M Bhaskaran. 2010. Palpatory method of measuring diastolic blood pressure. *Journal of anaesthesiology, clinical pharmacology* 26, 4 (2010), 528.

[87] A. Sapinski. 1992. Standard algorithm of blood-pressure measurement by the oscillometric method. *Medical and Biological Engineering and Computing* 30, 6 (1992), 671.

[88] Marianne Schroll and Ole Munck. 1981. Estimation of peripheral arteriosclerotic disease by ankle blood pressure measurements in a population study of 60-year-old men and women. *Journal of Clinical Epidemiology* 34, 6 (1981), 261–269.

[89] Jerome Segal. 1988. Blood flow measurement catheter. US Patent 4,733,669.

[90] N. Selvaraj, Y. Mendelson, K. H. Shelley, D. G. Silverman, and K. H. Chon. 2011. Statistical approach for the detection of motion/noise artifacts in Photoplethysmogram. In *2011 Annual International Conference of the IEEE Engineering in Medicine and Biology Society*. 4972–4975.

[91] Kirk Shelley and S Shelley. 2001. *Pulse Oximeter Waveform: Photoelectric Plethysmography.* 420–423.

[92] Steven W. Smith. 1997. *The Scientist and Engineer's Guide to Digital Signal Processing.*

[93] Frank D Stott. 1988. Blood pressure measurement. US Patent 4,730,621.

[94] Guocai Tao, Yan Chen, Changyun Wen, and Min Bi. 2011. Statistical analysis of blood pressure measurement errors by oscillometry during surgical operations. *Blood pressure monitoring* 16, 6 (December 2011).

[95] X. F. Teng and Y. T. Zhang. 2003. Continuous and noninvasive estimation of arterial blood pressure using a photoplethysmographic approach *(IEEE Engineering in Medicine and Biology Society)*. 3153–3156.

[96] M Todorovic, EW Jensen, and C Thøgersen. 1996. Evaluation of dynamic performance in liquid-filled catheter systems for measuring invasive blood pressure. *International journal of clinical monitoring and computing* 13, 3 (1996), 173–178.

[97] S. Tong, Z. Li, Y. Zhu, and N. V. Thakor. 2007. Describing the Nonstationarity Level of Neurological Signals Based on Quantifications of Time-Frequency Representation. *IEEE Transactions on Biomedical Engineering* 54, 10 (Oct 2007), 1780–1785.

[98] D Th Ubbink. 2004. Toe blood pressure measurements in patients suspected of leg ischaemia: a new laser Doppler device compared with photoplethysmography. *European journal of vascular and endovascular surgery* 27, 6 (2004), 629–634.

[99] Sakir Uen, Burkard Weisser, Paul Wieneke, Hans Vetter, and Thomas Mengden. 2002. Evaluation of the performance of a wrist blood pressure measuring device with a position sensor compared to ambulatory 24-hour blood pressure measurements. *American journal of hypertension* 15, 9 (2002), 787–792.

[100] Yuji Uenishi, Eiji Higurashi, Kazunori Naganuma, Shouichi Sudo, Junichi Shimada, Kimihisa Aihara, Hiroshi Koizumi, Naoe Tatara, Shoichi Hayashida, Shinji Mino, et al. 2010. Living body information detection apparatus and blood-pressure meter. US Patent App. 12/847,985.

[101] GA Van Montfrans, GM Van Der Hoeven, JM Karemaker, W Wieling, and AJ Dunning. 1987. Accuracy of auscultatory blood pressure measurement with a long cuff. *Br Med J (Clin Res Ed)* 295, 6594 (1987), 354–355.

[102] G. A. Van Montfrans. 2001. Oscillometric blood pressure measurement: progress and problems. *Blood pressure monitoring* 6, 6 (2001), 287–290.

[103] Bart W.A.M.M. Beulen, Nathalie Bijnens, Gregory G Koutsouridis, Peter Brands, Marcel C.M. Rutten, and Frans van de Vosse. 2011. Toward Noninvasive Blood Pressure Assessment in Arteries by Using Ultrasound. *Ultrasound in medicine biology* 37, 5 (May 2011), 788–797.

[104] Edward Jay Wang, Junyi Zhu, Mohit Jain, Tien-Jui Lee, Elliot Saba, Lama Nachman, and Shwetak N. Patel. 2018. Seismo: Blood Pressure Monitoring Using Built-in Smartphone Accelerometer and Camera. In *Proceedings of the 2018 CHI Conference on Human Factors in Computing Systems (CHI '18)*. 425:1–425:9.

[105] R. Wang, W. Jia, Z. Mao, R. J. Sclabassi, and M. Sun. 2014. Cuff-free blood pressure estimation using pulse transit time and heart rate. In *2014 12th International Conference on Signal Processing (ICSP)*. 115–118.

[106] S. Wassertheurer, J. Kropf, T. Weber, M. Van der Giet, J. Baulmann, M. Ammer, B. Hametner, CC. Mayer, B. Eber, and D. Magometschnigg. 2010. A new oscillometric method for pulse wave analysis: comparison with a common tonometric method. *Medical and Biological Engineering and Computing* 24, 8 (2010), 498–504.

[107] ST Yao, JT Hobbs, and WT Irivne. 1969. Ankle systolic pressure measurements in arterial disease affecting the lower extremities. *British Journal of Surgery* 56, 9 (1969), 676–679.

[108] S.A. Yarows, S. Julius, and T.G. Pickering. 2000. Home Blood Pressure Monitoring. *Arch Intern Med.* 160, 9 (May 2000), 1251–1257.